PHOTONIQUE MOLÉCULAIRE :
MATÉRIAUX, PHYSIQUE ET COMPOSANTS
MOLECULAR PHOTONICS: MATERIALS, PHYSICS AND DEVICES

Photoinduced multipolar tensorial patterning in polymer films by coherent control of molecular orientation

Sophie Brasselet [*], **Sébastien Bidault**, **Joseph Zyss**

Laboratoire de photonique quantique et moléculaire (UMR CNRS 8537),
Institut d'Alembert (IFR 121 / FR 2357), École normale supérieure de Cachan, 61, avenue du Président Wilson, 94235 Cachan, France

Abstract   Based on an early proposition by R.J. Glauber in 1967, the possibility to break centrosymmetry in molecular media by interference between one- and two-photon absorption pathways has been implemented in polymers throughout the last decade. This effect has been more recently advantageously generalized to optically induce adjustable multipolar molecular ordering in polymer thin films for nonlinear optics. A major benefit of this approach lies in the control of the final molecular orientational distribution by pure optical parameters such as phase or polarization of write beams. In this article, we extend a tensorial multipolar engineering experiment to encompass tensorial monitoring of photo-induced molecular orientational orders up to the 4th order. Coherent control of optical write beams, combined with real-time tensorial probing of optical properties in the material, provide access to a complete characterization of each excitation pathway contributing to the process. ***To cite this article: S. Brasselet et al., C. R. Physique 3 (2002) 479–492.*** © 2002 Académie des sciences/Éditions scientifiques et médicales Elsevier SAS

nonlinear optics / tensorial holographic storage / multipolar molecular engineering / SHG / THG

Photostructuration multipolaire microscopique dans les films polymères par contrôle cohérent de l'orientation moléculaire

Résumé   Issue d'une proposition de R.J. Glauber en 1967, l'utilisation de l'interférence entre deux chemins d'absorption à un et deux photons dans le but de briser la centrosymétrie d'un milieu moléculaire est apparue il y a une dizaine d'années. Cet effet a pu être généralisé de manière à induire des ordres orientationels moléculaires à symétrie multipolaire dans les films polymères pour l'optique non linéaire. Dans cet article, nous étendons le concept d'écriture tensorielle multipolaire à la lecture en temps réel des paramètres d'ordre tensoriels photo-induits jusqu'à l'ordre 4. Le contrôle cohérent des faisceaux optiques d'écriture, couplé à une lecture tensorielle des propriétés optiques induites dans le matériau,

---

[*] Correspondence and reprints.
   E-mail address: sophie.brasselet@lpqm.ens-cachan.fr (S. Brasselet).

optique non linéaire / stockage holographique d'informations tensorielles / ingénierie des molécules multipolaires / GSH / GTH

1. Introduction

Throughout the last decade, significant advances have been reported in the field of organic material engineering for nonlinear optics. Performances have increased based on improved nonlinear efficiencies of molecular structures and better control of symmetry properties at the molecular level, but also at the supra-molecular level, where nano-scale assemblies can be crucial to enhance or favor optical responses [1]. The development of complex molecular structures have opened the field to new ways for macroscopic engineering of nonlinear properties. A major motivation for such studies lies in the control of the polarization response of nonlinear excitations such as to exhibit, for instance, polarization independent response in organic media [2]. In order to answer this issue and take advantage of the multiple routes offered by molecular engineering, the control of molecular orientation has to adjust to the variety of degrees of freedom that are available at the molecular level, towards optimal light-matter coupling schemes [3]. In this perspective, the traditional electric field poling has been recently completed and sometimes advantageously replaced by optically assisted methods [4]. Purely optical interactions provide access to a new type of control of molecular matter at a macroscopic level, which involves spectroscopic properties of complex molecules, such as excited state symmetries as well as photo-physical and photo-chemical properties.

In this contribution, we present a purely optical scheme in order to gain control of molecular orientational distributions in polymer matrices. It is well known that one-photon excitation of chromophores induces a non-isotropic selective excitation that strongly depends on the electromagnetic field polarization. The field that is interacting with the molecules within the time frame of their re-orientational dynamics is indeed a nonzero time-averaged quantity $\langle |E|^2 \rangle_t$. If the selected set of pre-excited molecules bear the ability to re-orient through the relaxation process to their ground state, the accumulation of excitation cycles may asymptotically result in a permanent imprinting based on the so-called selective angular hole burning effect. This effect, also referred to as the Weigert effect, has been observed in polymer films doped with photo-isomerizable chromophores, excited by a linearly or circularly polarized resonant beam [5]. The molecular population that is predominantly excited follows an angular distribution of axial symmetry, which consequently induces an axial anisotropy in the linear optical response of the material, reflecting in birefringence and dichroïsm.

All-optical poling is a more recent technique that brings the advantage of inducing both centrosymmetric and non-centrosymmetric ordering contributions. This process combines two molecular excitation pathways, respectively excited at ω and 2ω, followed by relaxation pathways that allow for mechanical re-orientations of the molecular structure, such as resulting from reversible photo-isomerization processes. Each beam taken independently induces an axial Weigert-type effect on the angular redistribution of the molecular population. However, an additional contribution which imparts non-centrosymmetry to the medium can be singled-out. The origin of the non-centrosymmetric contribution to the selective angular hole-burning rests in coherent interference between single photon and two-photon absorption processes, which correspond to a nonzero cubic time averaged optical field $\langle E^3 \rangle_t$. The occurrence of such effect has been speculated by Glauber [6] and experimentally demonstrated for the first time by Osterberg and Margulis in silica fibers [7]. It was later accounted for in a phenomenological model by Baranova and Ya. Zel'dovich [8]. More recently, Fiorini and co-workers showed the possibility to use a similar excitation scheme in polymers doped with nonlinear chromophores, in order to induce a permanent photoinduced

non-linear macroscopic order [9]. The possibility to photo-induce multipolar orientational symmetries has been subsequently demonstrated [10] and lead to the introduction of tensorial product of write and read tensorial fields as photonic multipolar combination mirroring the multipolar symmetry of the molecule. The variety of molecular structures available for optical poling has also enriched the field allowing in particular to demonstrate optical poling of octupolar molecules [11], which are not amenable to electric field poling.

A broad variety of effects related to this scheme have been investigated in atomic physics, where quantum interferences between two excitation pathways have been observed by controlling the temporal delay between the two beams. Such phenomena, referred to as coherent control of excited states [12,13], allows for the use of the interference of the optical pumping fields towards time control of the excited state population and other features of atoms or small molecules in the gas phase. The excited state population is therefore built-up to reflect the quantum interference information. In a molecular medium at room temperature in the condensed phase, where optical linewidths are very broad, other ways of controlling molecular properties through the optical overall excitation mechanism can be thought of and derived from this scheme. Indeed in the all-optical poling scheme, the molecular re-orientation is driven by the relative amount of the one-photon, two-photon and interfering contribution to the excitation pathway. The relative phase shift and intensities of the coherent ω and 2ω beams are therefore actual control parameter for the final orientational pattern. Moreover, permanent imprinting of the excitation scheme within the medium also provides a way to store multiphotonic tensorial information, based on the field polarizations that have been used in the excitation process.

In this paper, we present all-optical poling as a possibility to engineer such polarized information storage in nonlinear multipolar molecular media. We will describe in the first part how coherent control of the one- and two-photon excitation schemes allows for the specific tailoring of centrosymmetric and non-centrosymmetric contributions to the orientational molecular distributions in a polymer film. In the second part, we show how to probe this tensorial information throughout the build-up of the orientational order: the characterization of photo-induced multipolar patterns is described by use of adequate tensorial read-out probes. We show in particular that third harmonic generation real-time monitoring comes to complement second-harmonic generation in order to provide orientationnal order parameters up to $J = 4$, thus providing a better insight onto the various dynamical molecular reorientation mechanisms at work in optical poling.

2. Coherent control of molecular orientational distributions

All-optical poling of nonlinear chromophores in polymer films is based on the interference between one- and two-photon excitation pathways, originating respectively from a strong incoming E^ω fundamental field and a weaker $E^{2\omega}$ second harmonic field. The excitation pathway from the ground state $|0\rangle$ to the excited states $|e\rangle$, assuming a two-level quantum system to depict molecular transitions, involves three distinct processes represented in Fig. 1: one-photon and two-photon absorption, with respective probabilities
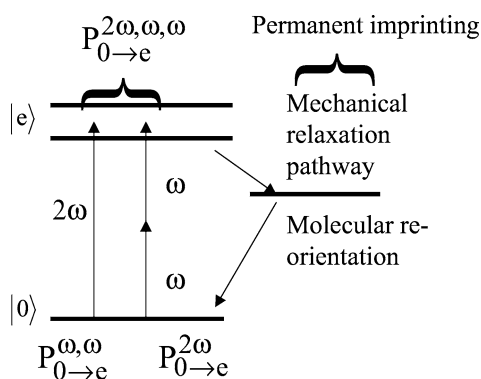
Figure 1. Excitation scheme following one- and two-photon resonant optical writing process in all-optical poling.

481

$P_{0 \to e}^{2\omega}(\Omega)$ and $P_{0 \to e}^{\omega,\omega}(\Omega)$, and coherent interferences between one- and two-photon excitations with a joint probability $P_{0 \to e}^{2\omega,\omega,\omega}(\Omega)$. The final stationary state reached at equilibrium after subsequent orientational relaxation, can be accounted for by an asymptotic anisotropic molecular orientational distribution $f(\Omega)$, where $\Omega = (\theta, \varphi, \psi)$ stands for the generalized Euler angular coordinates attached to a randomly oriented molecule. The orientational distribution $f(\Omega)$ results from contributions of each excitation process which participates to an angular hole burning process in the material [10]. The following normalized expression can be given for $f(\Omega)$:

$$f(\Omega) = \frac{1 - \phi_1 P_{0 \to e}^{2\omega}(\Omega) - \phi_3 P_{0 \to e}^{\omega,\omega}(\Omega) - \phi_2 P_{0 \to e}^{2\omega,\omega,\omega}(\Omega)}{\int \left(1 - \phi_1 P_{0 \to e}^{2\omega}(\Omega) - \phi_3 P_{0 \to e}^{\omega,\omega}(\Omega) - \phi_2 P_{0 \to e}^{2\omega,\omega,\omega}(\Omega)\right) \mathrm{d}\Omega} \tag{1}$$

where ϕ_1, ϕ_2 and ϕ_3 are the quantum efficiency of the one photon, two-photon excitation-reorientation process and joint excitation, respectively. These factors, being of similar order of magnitude, represent mainly cumulated photoisomerization quantum yields. In the following calculations, we will denote Λ the normalization coefficient appearing at the denominator in this expression.

In order to single-out symmetry features in the orientational distribution function, it is convenient to expand it on the basis of Wigner rotation matrix coefficients $D_{m'm}^J(\Omega)$ [14], namely $f(\Omega) = \sum_{m',m,J} f_{m'm}^J D_{m'm}^J(\Omega)$, with the set of $f_{m'm}^J$ coefficients unambiguously defining the molecular orientational distribution. We will further discuss the possibility to infer these coefficients from experiments.

In the configuration investigated in this work, the dynamical tailoring of the $f(\Omega)$ distribution originates from a resonant molecular-field coupling process and therefore depends on the excitation fields and molecular polarizabilities involved in the multiphotonic excitations. Consequently, in order to determine the $f_{m'm}^J$ coefficients, it is necessary to specify the different symmetry features of the excitation probabilities.

The excitation probabilities from the ground $|0\rangle$ to the excited states $|e\rangle$ can be inferred from the resonant excitation of a non-linear chromophore by the sum of the E^ω and $E^{2\omega}$ fields [10]:

$$P_{0 \to e}^{2\omega}(\Omega) \propto \alpha_{\mathrm{w}}(-2\omega; 2) \bullet \left\langle E^{2\omega^*} \otimes E^{2\omega} \right\rangle_t + \text{c.c.},$$

$$P_{0 \to e}^{\omega,\omega}(\Omega) \propto \gamma_{\mathrm{w}}(-\omega; -\omega, \omega, \omega) \bullet \left\langle E^{\omega^*} \otimes E^{\omega^*} \otimes E^{\omega} \otimes E^{\omega} \right\rangle_t + \text{c.c.},$$

$$P_{0 \to 1}^{2\omega,\omega,\omega}(\Omega) \propto \beta_{\mathrm{w}}(-2\omega; \omega, \omega) \bullet \left\langle E^{2\omega^*} \otimes E^{\omega} \otimes E^{\omega} \right\rangle_t \mathrm{e}^{\mathrm{i}(\Delta kz + \Phi)} + \text{c.c.}, \tag{2}$$

where α_{w}, β_{w} and γ_{w} are 'write' polarizability tensors expressed here at the sum frequency for a given optical interaction. The joint probability exhibits a distinctive phase term with $\vec{\Delta k} = \vec{k}^{2\omega} - 2\vec{k}^\omega$ the phase mismatch wave vector between the ω and 2ω fields and $\Phi = \Phi^{2\omega} - 2\Phi^\omega$ their relative phase shift, z being along the propagation direction.

Expressions (2) originate from a perturbative treatment where the quantum mechanical interaction term is given by the usual dipolar coupling potential $-\vec{\mu} \cdot (\vec{E}^\omega + \vec{E}^{2\omega})$. The magnitude of each probability obviously depends on the field strengths and molecular polarizabilities. The 'write' tensors have been shown to be proportional to the resonant part of the molecular polarizabilities $\alpha(-2\omega; 2\omega)$ (one-photon absorption at 2ω, associated to the linear polarization), $\beta(-2\omega; \omega, \omega)$ (joint one- and two-photon, associated to the quadratic hyperpolarizability), and $\gamma(-\omega; -\omega, \omega, \omega)$ (two-photon absorption at ω associated to the cubic hyperpolarizability). Expressions of such tensors can be found in [15] for general molecular symmetries, such as multipolar planar structures, where a three-level model is needed to account for 2D tensorial properties. In this more general 3-level scheme, both excited states are taken in resonance with the write fields.

Expressions (2) single out the combined excitation probability as being the only one sensitive to the phase shift between the excitation fields, implying that this term will be the only one to reflect the coherent interference between the write beams. This combined term, being associated with the third-order β tensor, opens-up the possibility of a non-centrosymmetry contribution to the orientational distribution. In this work,

we will describe thin polymer films of thickness smaller than the coherence length of the nonlinear process and therefore ignore the Δkz dependence.

The expression for excitation probabilities are expressed in a compact form by use of contracted tensorial products, which readily lend themselves to the implementation of the general rotationally invariant spherical formalism. As is well known, this formalism is the relevant one to keep track of molecular symmetry features throughout eventually complex sequences of statistically distributed rotation operations. In this scheme, a nth order tensor T is expanded on the basis of the reduced spherical harmonics C_m^J, according to $T = \sum_{m, J \leqslant n} T_m^J C_m^J$ [16]. This tensorial basis appears to be particularly relevant in the more general context of multipolar molecular symmetries [17]. In the present work, we apply this decomposition to the 'write' tensor $\sigma_w^{(n)}$ associated with the nth order molecular polarizability $\sigma^{(n)}$, with $n = 1$–3, and the corresponding coupled field $E^{(n)}$. This notation allows us to treat the three different processes in Eq. (1) according to similar tensorial expressions albeit with different ranks n. Expressing $\sigma_w^{(n)}$ in the same macroscopic framework as the write fields, the contracted tensorial product can be written [16] as

$$\sigma_w^{(n)} \bullet E^{(n)} = \sum_{J, m, m'} \left(\sigma_w^{(n)}\right)_m^J D_{mm'}^J(\Omega)\left(E^{(n)}\right)_{m'}^{J*} \tag{3}$$

with the write field tensors defined respectively as

$$E^{(1)} = \left\langle E^{2\omega*} \otimes E^{2\omega} \right\rangle_t + \text{c.c.}, \qquad E^{(2)} = \left\langle E^{2\omega*} \otimes E^{\omega} \otimes E^{\omega} \right\rangle_t e^{i(\Delta kz + \Phi)} + \text{c.c.} \quad \text{and}$$

$$E^{(3)} = \left\langle E^{\omega*} \otimes E^{\omega*} \otimes E^{\omega} \otimes E^{\omega} \right\rangle_t + \text{c.c.}$$

Introducing the definition of $f(\Omega)$ and the orthogonality of Wigner matrix elements, the $f_{m'm}^J$ coefficients take the following expressions:

$$f_{m'm}^J = \frac{1}{\Lambda}\left(\delta_{m'=0}\delta_{m=0}\delta_{J=0} - p_1(a_w)_{m'}^J\left(e^{(1)}\right)_m^{J*} - p_2(b_w)_{m'}^J\left(e^{(2)}\right)_m^{J*} - p_3(c_w)_{m'}^J\left(e^{(3)}\right)_m^{J*}\right) \tag{4}$$

$$\text{where} \quad p_1 = \phi_1\|\alpha_w\|\left|E^{2\omega}\right|^2, \quad p_2 = \phi_2\|\beta_w\|\left|E^{2\omega}\right|\left|E^{\omega}\right|^2 \quad \text{and} \quad p_3 = \phi_3\|\gamma_w\|\left|E^{\omega}\right|^4.$$

These coefficients, which will be extensively used is what follows, are the relative strengths of the excitation–reorientation processes ($p_1, p_2, p_3 \leqslant 1$), which include the quantum efficiency of the phenomenon (ϕ_n) and the norms of the tensors $\|\sigma_w^{(n)}\|$ and $\|E^{(n)}\|$. In expression (4), $(s_w^{(n)})_m^J$ ($s = a, b$ or c) and $(e^{(n)})_m^J$ are the normalized spherical components of $\sigma_w^{(n)}$ and $E^{(n)}$, with $(s_w^{(n)})_m^J = (\sigma_w^{(n)})_m^J/\|\sigma_w^{(n)}\|$. The advantage of using normalized expressions is that the experimental determination of tensorial symmetries calls only on ratios of the corresponding spherical components, as will be developed in the next section. Absolute determination of the p_1, p_2, and p_3 quantum yield amplitude parameters is however possible, from the knowledge of the ω and 2ω energies and the magnitude of the molecular polarizabilites. Amplitude parameters p_1, p_2, and p_3 are furthermore linked to each other by the following relationships:

$$p_2^2 = p_1 \cdot p_3 \cdot \left[\frac{\phi_2^2}{\phi_1 \cdot \phi_3} \cdot \frac{\|\beta_w\|^2}{\|\alpha_w\|\|\gamma_w\|}\right], \qquad p_1 + p_2 + p_3 = C. \tag{5}$$

The first expression derives from the elimination of the field amplitudes between expressions p_1, p_2, and p_3, and reflects the balance between the different contributions of the overall excitation probability. The second relation is an overall probability closure condition and provides, via the sum C, the amount of molecules promoted into the excited states. In particular, $C = 1$ when the excitation process reaches saturation after equilibrium and assuming that no competitive relaxation process is involved. Expression (5) allows one to obtain p_2 from p_1 and p_3. These expressions lead furthermore to the conclusion that the joint probability effect that breaks non-centrosymmetry in the medium is maximum when the two other
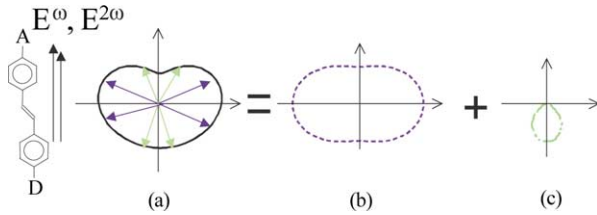
Figure 2. In-plane projection of the molecular orientation distribution for a rod-like molecule and two parallel writing beams, calculated for $p_1 = p_2 = p_3 = 0.2$. (a) represents the cylindrical symmetry $f(\theta)$ distribution function; (b) centrosymmetric part (even-J order parameters) of $f(\theta)$; and (c) antisymmetric part (odd-J order parameters) of $f(\theta)$.

processes are balanced, namely $p_1 = p_3$. The saturation condition ($C = 1$) leads to $p_1 = p_2 = p_3$, which can be obtained only in particular energy/polarizability conditions [9,18].

Expression (4) shows that the $f_{m'm}^J$ coefficients are jointly governed by the symmetry of the write fields $E^{(n)}$ as well as that of the molecular tensors $\sigma^{(n)}$. The maximum J order originates from the 4th order interaction process $\gamma \bullet E^{(4)}$, and is thus $J = 4$. Each interaction is weighted by the corresponding relative efficiency factor p_1, p_2, or p_3. Note that the number of $f_{m'm}^J$ coefficients can be considerably reduced in some particular write field symmetry configurations.

In order to discuss the symmetry features of the macroscopic optical response of the molecular orientational distribution, it is convenient to distinguish centrosymmetric and non-centrosymmetric contributions to the overall angular distribution $f(\Omega)$. We will denote $f_s(\Omega)$ and $f_a(\Omega)$ the symmetric and antisymmetric parts of $f(\Omega)$, which correspond respectively to even and odd J orders. The Wigner expansion of the symmetric part, namely $f_s(\Omega) = (f(\Omega) + f(\Omega + \pi))/2$, contains only even J orders, whereas the non-centrosymmetric projection, $f_a(\Omega) = (f(\Omega) - f(\Omega + \pi))/2$, will contain only odd J orders. A representation of these functions is provided in Fig. 2 in the particular case of a strong molecular dipole, as in the case of a 'rod-like' molecule, interacting with parallel E^ω and $E^{2\omega}$ polarizations. $f(\Omega)$ is therefore independent of the Euler angles ψ and φ, due to the cylindrical symmetry of the molecule. The cylindrical symmetry $f(\theta)$ function is plotted in Fig. 2 as obtained from a direct quantum mechanical calculation of the excitation probabilities. As shown in Fig. 2, the odd (Fig. 2(b)) and even (Fig. 2(c)) contributions to $f(\theta)$ correspond to the axial and polar parts of this function, each of them being weighted by the efficiency of the corresponding interaction process.

It is indeed convenient to single-out the odd and even contributions to $f(\Omega)$ as they can be separately probed by corresponding odd or even read-out processes. This can be generalized to any J component of $f(\Omega)$ in the Wigner expansion where individual $f_{m'm}^J$ projections can be probed by adequate J order read-out processes. In either case, the photo-orientation of molecules in a polymer film results in a strong change in the symmetry of the macroscopic polarisabilities.

The optical properties of the polymer film are traditionnally expressed in terms of the nth order tensor polarizability $\chi^{(n)}$, which is obtained from the corresponding nth order molecular polarizability by

$$\chi^{(n)} = \int_\Omega \sigma^{(n)}(\Omega) f(\Omega)\, d\Omega \tag{6}$$

where $\sigma^{(n)}(\Omega)$ is expressed in the macroscopic framework. A general and convenient way to express these quantities is based on the rotationally invariant spherical formalism, with $\chi^{(n)} = \sum_{m, J < n} (\chi^{(n)})_m^J C_m^J$ at the macroscopic level. Applying again the orthogonality properties of Wigner matrix elements, the spherical components of $\chi^{(n)}$ can be expressed as [10]

$$\left(\chi^{(n)}\right)_m^J = \frac{N}{2J + 1} \sum_{m'} \left(\sigma^{(n)}\right)_{m'}^{J*} f_{m'm}^J, \tag{7}$$

where N is the molecular density in the medium.

This general expression shows that the symmetry of the macroscopic orientational order has a strong influence on the symmetry of the macroscopic polarizabilities, and therefore on the linear and nonlinear anisotropy of the polymer film at any interaction order. We will more specifically explore in this context the case of first, second and third-order polarizabilities. The different macroscopic polarizabilities are in essence signatures of the different symmetry features in the molecular angular distribution. In particular, odd-order macroscopic polarizabilities $\chi^{(1)}$ and $\chi^{(3)}$ involve coupling between odd-order microscopic tensors (α and γ) and the distribution function $f(\Omega)$, thus filtering its rotational spectrum to even order terms as sustained by the $f_{m'm}^J$ coefficients with $J = 0, 2, 4$. Similarly, the even order $\chi^{(2)}$ polarizability couples the microscopic tensor β to odd order components $J = 1, 3$. However, in the most general symmetry case and close to resonances, pseudo-tensorial components such as $\beta^{J=2}$ or $\gamma^{J=1,3}$ may be non-negligible, due to break-up of Kleinman index permutation symmetry. These terms will therefore involve contributions from even or odd J orders in the $\chi^{(2)}$ or $\chi^{(3)}$ rotational expansion, respectively. The existence of these terms is however discarded in this work, where we consider only molecular symmetries that strictly cancel such components. The effect of these components when exciting multipolar molecules nearby optical resonances will be detailed in a future contribution [18].

Based on the experimental determination of the $(\chi^{(n)})_m^J$ spherical contributions to be discussed in the next section, it becomes possible to infer the macroscopic $f_{m'm}^J$ order parameters from the knowledge of independently measured molecular polarizabilities. Expression (7) exemplifies the broad variety of macroscopic polarizability symmetry types which are available from adequate poling configurations, by playing on the molecular structures or in a more subtle way, the symmetry features of the write field and molecular polarizability tensors [10,19]. This underlying flexibility provides many openings in terms of holographic data storage of tensorial information with an increased number of control parameters at hand. In the following section, the tensorial nature of the read-out process will be more specifically investigated, as a way to sort-out the symmetry feature of the all-optically engineered $f(\Omega)$ orientation distribution function.

3. Multi-photonic probes of multipolar molecular order in a polymer matrix

Experimental determination of the symmetry of the $\chi^{(n)}$ susceptibility tensors following the all-optical poling step is performed by probing the encoded medium by an adequate set of read fields. Nonlinear optical interactions provide an ideal context to access molecular distributions of different symmetry properties. In this part, we show how to access to spherical components of the macroscopic polarizability coefficients. Calling on interactions of increasing order allows in particular to access only to statistical moments of the $f(\Omega)$ distribution of increasing orders. Since odd-order hyperpolarisabilities ($\chi^{(1)}, \chi^{(3)}, \dots$) relate only to even order components of $f(\Omega)$, such techniques as anisotropic one- and two-photon absorption or third harmonic generation (THG) anisotropy will permit to depict the molecular distribution $f_s(\Omega)$. In order to complement the determination of even order parameters, three wave mixing read-out technique such as second harmonic generation (SHG) will permit access to odd orders related to $f_a(\Omega)$.

In order to represent the read-out process for a given symmetry order, a 'read' tensor $F^{(n)}$ needs to be recalled. The concept of read tensor had been first introduced in order to take fully advantage of a rotationally invariant tensor decomposition accounting for optical-matter interactions [20,21]. The nth order read-out process consists in the specific measurement of the nth order macroscopic polarizability $\chi^{(n)}$, with $I^{m\omega_r} = |\chi^{(n)} \bullet F^{(n)m\omega_r}|^2$ being the out-going nth harmonic at frequency $m\omega_r$ ($n = m$ in the sum frequency case), with an incoming frequency at ω_r. The read tensor can be expressed as $F^{(n)m\omega_r} = e^{m\omega_r} \otimes E^{\omega_r} \otimes \cdots \otimes E^{\omega_r}$, where E^{ω_r} is the read incident beam and $e^{m\omega_r}$ represents the direction of the detected polarization vector.

In usual cases for real-time monitoring of all-optical poling experiments, the poled sample is probed by a read beam at either 2ω (one-photon absorption) or ω (SHG, THG and two-photon absorption), making therefore use of the same frequencies as for the write process. In the case of a nth order read-out scheme,

the intensity is therefore

$$I^{m\omega_r} = \left| \sum_{m,J} \left(\chi^{(n)}\right)^J_m \left(F^{(n)}\right)^{J^*}_m \right|^2 = \left| \sum_{m,m',J} \frac{N}{2J+1} \left(\sigma^{(n)}\right)^{J^*}_{m'} f^J_{m'm} \left(F^{(n)}\right)^{J^*}_m \right|^2 \tag{8}$$

with the same notations as in the previous section.

Inspection of expression (8) shows that the knowledge of the molecular hyperpolarizability together with the combination of read fields can provide direct access to the $f^J_{m'm}$ order parameters defining the optically poled medium either in real time or when steady state is reached. Properties of the read-out tensor are detailed in [10] in the $n = m = 2$ case for second harmonic generation (SHG) measurements. We shall attempt to generalize these results hereafter.

In order to identify the molecular distribution coefficients $f^J_{m'm}$ using the read tensor properties, we chose to measure the anisotropy of the nth order intensities with $n = 1$ to 3 at $\omega_r = \omega$. In the following experiments, the polarization of the probe beam is made to rotate in the plane of the sample. Denoting (X, Y) the sample plane, which is orthogonal to the propagation direction, the read-out polarization is then defined by an angle $\varphi = (X, E^\omega)$ in the transverse plane. The analysis direction being defined by the unit vector $e^{n\omega}$, the read tensor is therefore $F^{(n),n\omega}(\varphi) = e^{n\omega} \otimes E^\omega(\varphi) \otimes \cdots \otimes E^\omega(\varphi)$ with $E^\omega(\varphi) = E^\omega(\cos\varphi \vec{X} + \sin\varphi \vec{Y})$.

As pointed-out in the previous section, the odd and even order intensities single-out distinct features that depend both on the molecular symmetry and on the write field symmetry. Using expressions (4) and (6) in the case of $n = 2$, the SHG intensity can be further simplified [10]:

$$I^{SHG}(\varphi) = I^{2\omega}(\varphi) \propto \|\beta\|^2 \left| \sum_{J=1,3} \frac{Np_2 \cos(\Delta kz + \Phi)}{2J+1} (b_w \bullet b)^J \left(e^{(2)} \bullet F^{(2)}(\varphi)\right)^J \right|^2 \tag{9}$$

with the notation $(T \bullet U)^J = \sum_m T^J_m U^{J^*}_m$ [11], and Φ, Δkz and p_2 as defined in the previous section. In this expression, $F^{(2)2\omega}(\varphi) = e^{2\omega} \otimes E^\omega(\varphi) \otimes E^\omega(\varphi)$ is the SHG read field tensor. We can furthermore expand the nonlinear write and read tensors using the expression $(b_w \bullet b)^J = \|b^J\|^2$, which is justified close to resonance [15].

Expression (9) shows that for even order $n = 2$ processes, which are the most widely studied in the litterature, nonlinear anisotropies that are entirely dependent on the molecular and write field symmetries can be read-out [10,11]. It appears indeed from expression (9) that both the p_2 interfering efficiency term and the phase shift term are not affecting the symmetry of the SHG response in the thin film, but only its magnitude.

Second harmonic generation is therefore an interesting scheme entailing the advantage of giving information on the molecular β symmetry from the sole knowledge of the write field tensor symmetry. The $(E^{(n)})^J_m$ contributions can be engineered by adequate combinations of write polarizations, as detailed in [10], with circular polarizations playing a particular role as they sustain purely $J = 1$ (co-circular) and $J = 3$ (counter-circular) tensors. Such dependence has been advantageously used in order to photo-induce non-centrosymmetric orders in polymer media containing molecules of various symmetry. The benchmark experiment in this respect was the first illustration of all-optical poling of octupolar molecules [11].

In order to express the SHG dependence with respect to such factors, the most relevant experimental parameter is the nonlinear SHG anisotropy $I^{SHG}_\perp / I^{SHG}_\|$. It represents the ratio between the SHG intensity measured for a read ω polarized in the direction perpendicular to the write ω polarization (noted $\perp$), and the direction parallel to the write ω polarization (noted $\|$).

This quantity is plotted in Fig. 3 for linearly polarized parallel write beams, as a function of the molecular anisotropy $\|\beta^3\|/\|\beta^1\|$, ranging from 0 (dipolar molecule) to 15 (quasi-octupolar molecule). The insets are polar plots of the φ dependence of $I^{SHG}(\varphi)$ for various molecular symmetry types. It appears that such
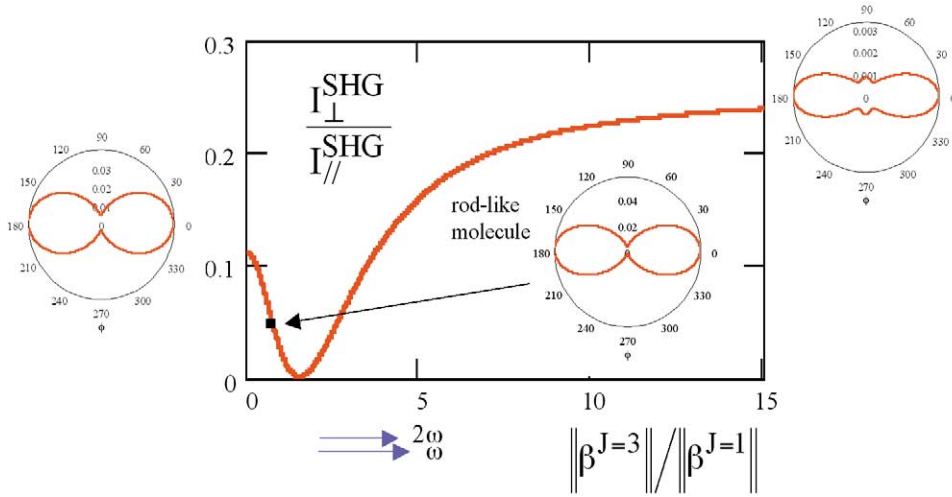
Figure 3. SHG intensity in-plane anisotropy as a function of the molecular spherical anisotropy, in the case of parallel write linear polarizations. For $\|\beta^{J=3}\|/\|\beta^{J=1}\| \leqslant 15$, the molecular symmetry ranges from purely dipolar to quasi-octupolar. $I_{\perp}^{\text{SHG}}$ stands for the SHG intensity measured in the perpendicular direction to the ω writing polarization, and $I_{\|}^{\text{SHG}}$ to the parallel direction. The insets are the corresponding angular responses in polar plot representations for a variable read-out linear polarization angle in the transverse plane.

an experiment is only sensitive to molecular symmetry in the anisotropy ratio range $\|\beta^3\|/\|\beta^1\| \leqslant 10$. Polar plots in Fig. 3 show that the SHG anisotropy is not strongly sensitive to the molecular anisotropy. However, unambiguous signatures of deviations of the molecular symmetry from the pure dipolar case can be obtained.

Other write tensor symmetries, resulting from different sets of polarizations such as orthogonal ones, allow one to cover a broader range of molecular anisotropies [10,19]. However, when the write fields polarizations are circular, the SHG anisotropy is independent of the molecular symmetry, which can be of great interest for applications. Indeed, when the polarizations are contra-circular, the write field tensor is purely $J = 3$ in symmetry, which is then coupled to the sole $\beta^{J=3}$. Therefore, the SHG intensity increases with the octupolar $\beta^{J=3}$ magnitude but its symmetry remains the same. Similarly, in the co-circular configuration, the write fields tensor is purely $J = 1$ and is thus coupled to $\beta^{J=1}$ only, resulting in a constant anisotropy. Elliptical polarizations, being intermediate cases, do not provide additional informations, as already pointed-out in [10,19].

An identical formalism is applied in the following to one-photon absorption (OPA), third harmonic generation (THG) and two-photon absorption (TPA). In the case of one-photon absorption at 2ω, the outgoing intensity is related to the $\chi^{(1)}(-2\omega; 2\omega)$ tensor, with

$$I^{\text{OPA}}(\varphi) = \|\alpha\|^2 \left| \sum_{J=0,2} \frac{1}{2J+1} \left(a_0^0 \left(F^{(1)2\omega}(\varphi) \right)_0^0 - p_1 \|a^J\|^2 \left(e^{(1)} \bullet F^{(1)2\omega}(\varphi) \right)^J \right. \right.$$

$$\left. \left. - p_3 (\gamma_{\text{w}} \bullet a)^J \left(e^{(3)} \bullet F^{(1)2\omega}(\varphi) \right)^J \right) \right|^2 \tag{10}$$

where $\alpha_{\text{w}} = \alpha = \alpha(-2\omega; 2\omega)$ for similar reasons as in expression (9), and $F^{(1)2\omega}(\varphi) = e^{2\omega} \otimes E^{2\omega}(\varphi)$ being the one-photon absorption read field tensor. The first order optical process clearly depends on even orders of the molecular symmetry which govern the polarizability coefficients $\alpha^{J=0,2}$. Contrary to the previous

SHG configuration, the OPA anisotropy depends on the relative efficiencies of the one- and two-photon absorption processes which are accounted for in the p_1 and p_3 parameters defined in Section 2.

In the THG case where the frequency 3ω is being generated, the measured intensity is related to the $\chi^{(3)}(-3\omega, \omega, \omega, \omega)$ polarizability and can be expressed as

$$I^{\mathrm{THG}}(\varphi) = \|\gamma\|^2 \left| \sum_{J=0,2,4} \frac{1}{2J+1} \left(c_0^0 \left(F^{(3)3\omega}(\varphi) \right)_0^0 - p_1 (a_{\mathrm{w}} \bullet c)^J \left(e^{(1)} \bullet F^{(3)3\omega}(\varphi) \right)^J \right. \right.$$

$$\left. \left. - p_3 \|c_J\|^2 \left(e^{(3)} \bullet F^{(3)3\omega}(\varphi) \right)^J \right) \right|^2 \tag{11}$$

where $\gamma = \gamma^{\mathrm{THG}} = \gamma(-3\omega; \omega, \omega, \omega)$ stands for the THG microscopic tensor, $\gamma = \gamma(-\omega; -\omega, \omega, \omega)$ the two-photon absorption microscopic tensor and $F^{(3)3\omega}(\varphi) = e^{3\omega} \otimes E^\omega(\varphi) \otimes E^\omega(\varphi) \otimes E^\omega(\varphi)$ is the THG read field tensor.

The case of two-photon absorption (TPA) read-out configuration, where the $\chi^{(3)}(-\omega, \omega, \omega, -\omega)$ tensor is being measured, provides an intensity expression similar to (11), with $\gamma = \gamma_{\mathrm{w}} = \gamma^{\mathrm{TPA}} = \gamma(-\omega; -\omega, \omega, \omega)$ and $F^{(3)\omega}(\varphi) = e^\omega \otimes E^{\omega*}(\varphi) \otimes E^\omega(\varphi) \otimes E^\omega(\varphi)$ is the TPA read field tensor.

These processes, either one-photon, two-photon absorption or THG, are therefore allowing to access the even order parameters of the molecular distribution $f(\Omega)$ up to $J = 4$. Contrary to SHG, the relative strength of the one- and two-photon excitation processes (p_1/p_3) may strongly affect the anisotropy of these signals. This supports the fact that the shape of $f_{\mathrm{s}}(\Omega)$, the centrosymmetric part of $f(\Omega)$, is strongly dependent on the relative efficiency of one- and two-photon excitations. Moreover, variations of the molecular or write field symmetries may also affect the anisotropy, but less efficiently than for $f_{\mathrm{a}}(\Omega)$. The effect of the write field symmetry is indeed quite different from that in the SHG case. For circularly polarized write fields, $f_{\mathrm{s}}(\Omega)$ will be perfectly isotropic in the sample plane since all the excited molecules will reorient perpendicularly to this plane. For linearly polarized perpendicular fields, one- and two-photon absorption counterbalance one another and the distribution is almost completely isotropic in the sample plane. The most illustrative configuration is obtained with parallel write polarizations, whereby the photo-induced distribution displays cylindrical symmetry around the write fields polarizations direction. Moreover, this configuration favors the highest anisotropy in $f_{\mathrm{s}}(\Omega)$.

In order to obtain a better understanding of the p_1/p_3 dependence of $f_{\mathrm{s}}(\Omega)$, we will henceforth focus on a rod-like molecule such as Disperse Red 1. Such molecular symmetry presents the advantage of sustaining both dipolar and octupolar β components, with a constant anisotropy ratio $\|\beta^3\|/\|\beta^1\| = \sqrt{3/2} = 0.81$ [18], leading to simple analytical forms of the spherical tensorial expressions. Indeed, as the only considered Cartesian components of the polarizability tensors are $\alpha_{zz} \gg (\alpha_{xx}, \alpha_{yy})$, β_{zzz}, and γ_{zzzz}, with z along the dipole direction, the $(\sigma^{(n)})_m^J$ spherical coefficients reduce to $m = 0$ for each J. The spherical components of the molecular polarisabilities are then:

$$\alpha_0^0 = -\frac{1}{\sqrt{3}} \alpha_{zz}, \qquad \alpha_0^2 = \frac{2}{\sqrt{6}} \alpha_{zz}, \qquad \beta_0^1 = \sqrt{\frac{3}{5}} \beta_{zzz}, \qquad \beta_0^3 = \frac{2}{\sqrt{10}} \beta_{zzz},$$

$$\gamma_0^0 = \frac{1}{\sqrt{5}} \gamma_{zzzz}, \qquad \gamma_0^2 = \frac{-2}{\sqrt{7}} \gamma_{zzzz}, \qquad \gamma_0^4 = \frac{4}{\sqrt{70}} \gamma_{zzzz}. \tag{12}$$

Note that this symmetry and shape feature allow for index permutations even in the resonant case, as a single z index is participating. The relative values of spherical components of γ^{THG} and γ^{TPA} are therefore equal while their norms are different. Consequently, the experimental two-photon absorption and THG intensity anisotropies are equal and will be denoted $(I_\perp/I_\parallel)^{\mathrm{THG,TPA}}$. For the same reason the $\beta^{J=0,2}$ and $\gamma^{J=1,3}$ coefficients vanish even in resonant conditions, whereas these coefficients might be otherwise significant for general molecular symmetries [12,13].
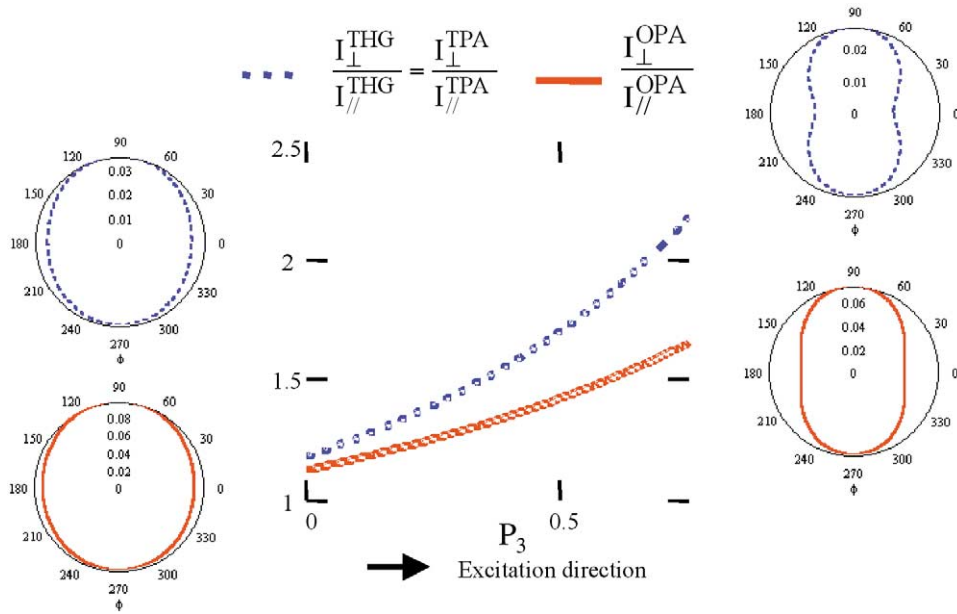
Figure 4. THG and one- (OPA) and two-photon (TPA) absorption intensities in-plane anisotropy as a function of the strength p_3 of the two-photon excitation efficiency, in the case of writing beams with parallel linear polarizations, for $p_1 = 0.25$. The insets are the corresponding angular responses for a variable read-out linear polarization.

In the following, the write fields polarizations are chosen linear and parallel, such as in the write configuration of Fig. 3. Figure 4 represents the p_3 dependence of the THG/TPA and one-photon absorption $(I_\perp^{OPA}/I_\parallel^{OPA})$ anisotropies for $p_1 = 0.25$. Note that when $p_3 = 0$ (ω beam off), the write configuration corresponds to the well-known Weigert effect, with a very slight evidence of anisotropy in the φ dependence of this signal (see inset). Figure 4 shows that the THG/TPA anisotropy change with increasing p_3 is more important than the one-photon absorption case. This results from the more restrictive symmetry feature of one-photon absorption which contains only $J = 0, 2$ components of $f_s(\Omega)$ whereas THG/TPA signals may include additional $J = 4$ components. It is therefore necessary to include optical mixing phenomena involving at least four waves processes in order to probe the complete centrosymmetric part up to $J = 4$.

4. Experimental study

Experimental studies have been conducted on grafted DR1/polymethymetacrylate (PMMA) polymer thin films (5% w/w of DR1), deposited by the spin-coating technique. The maximum absorption wavelength of this sample is $\lambda_{max} = 488$ nm. The resulting optical density at 532 nm is approximately 1. Therefore, the 532 nm and 1.064 μm write wavelengths can be used for one- and two-photon absorption processes. An experimental co-propagating configuration was implemented for the one- and two-photon excitation processes, as sketched in Fig. 5. The fundamental IR laser source at 1.064 μm is a single-mode Nd^{3+}:YAG laser with pulses of 22-ps duration at a 10-Hz repetition rate. The $E^{2\omega}$ harmonic write field is generated by frequency doubling of the incident E^ω fundamental field in a type-II phase-matched KDP crystal. $E^{2\omega}$ and E^ω are linearly polarized with parallel directions using a Glan polarizer. The fundamental power equals $1.5 \cdot 10^{12}$ W/cm^2 for a 300 μm diameter at beam waist. The E^ω field was also used as a read beam, with a half-wave plate to rotate the polarization. The probing techniques were SHG and THG, measured along the write fields propagation direction as defined by the wave-vector matching conditions. The SHG and THG signals were split using a dichroic mirror at 420 nm, allowing the signals to be measured simultaneously
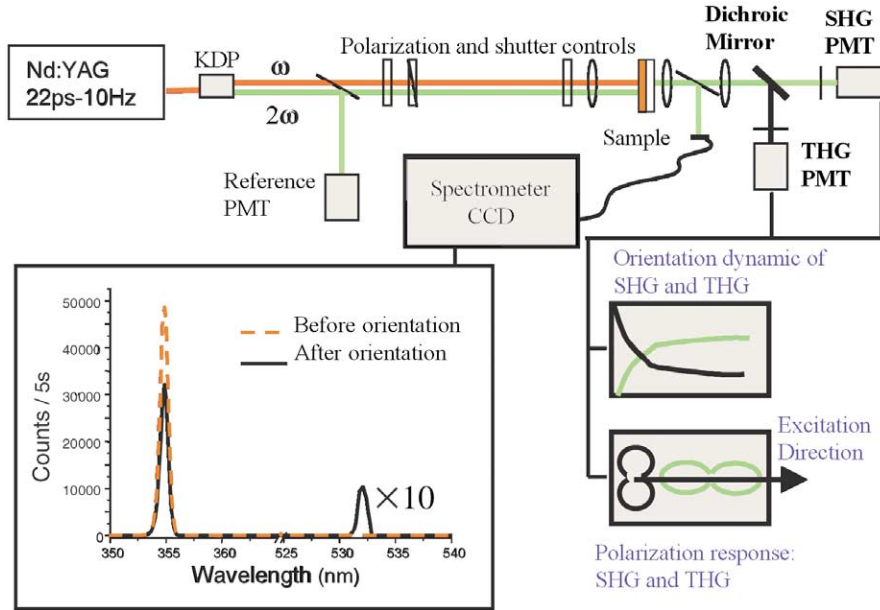
Figure 5. Experimental set-up for a bi-photonic excitation scheme with read-out by second harmonic (SHG) and third harmonic (THG) generation (see text for description). Inset: spectrum of emission showing THG and SHG spectra before and after the all-optical poling of DR1 molecules in a grafted DR1-PMMA polymer (5% w/w).

by use of two PMTs. The dynamics of the orientation is sketched in Fig. 5, showing the existence of a non-centrosymmetric stationary state. The spectral signature of the intensities was measured using a spectrometer coupled to a fibered CCD camera. The SHG signal is much lower than the THG signal (by more than one order of magnitude). This situation reflects the lower number of molecules participating to the build-up of the non-centrosymmetric distribution $f_a(\Omega)$, while all chromophores take part in the THG intensity. However, the onset of SHG is clearly visible from a zero initial background, whereas variations of the stronger THG signal can be more elusive. These spectra show the onset of SHG and the decrease of THG in the field's polarization direction.

When equilibrium was reached in the orientation process, the photoinduced SHG and THG anisotropies were measured, as represented in Fig. 6. The THG technique was chosen preferentially as compared to TPA for wavelength detection reasons. The theoretical fit of the SHG anisotropy gives for DR1 a molecular anisotropy ($\|\beta^3\|/\|\beta^1\|$) close to 0.45 which is quite far from the theoretical value of 0.81. However, as seen in Fig. 3, the SHG dependence on the read-out angle φ is weakly sensitive to the molecular symmetry when the write fields are parallel. Other write field configurations provide more reliable configurations to measure precisely the molecular anisotropy, as discussed earlier. The specific use of all-optical poling for determining molecular symmetry properties is discussed in [10].

THG responses are much less anisotropic than SHG, as seen in Figs. 3(a) and 3(b). Higher experimental THG anisotropies have been observed in situations where the anisotropic photodamage in the material was non-negligible [22]. However such situation does not lend itself to experimental quantitative evaluation of the $f(\Omega)$ parameters. In the present context, fitting the THG anisotropy allowed to determine the relative amount of one- to two-photon absorption efficiencies, leading respectively to $p_1 = 0.17$ and $p_3 = 0.27$. Figure 6(c) shows the theoretical fit of the photoinduced THG anisotropy compared to the initially isotropic THG. The resulting $f_s(\Omega)$ function after orientation still remains quite isotropic, in agreement with the previous remarks. The experimental p_1 and p_3 values show one- and two-photon excitation efficiencies rather equilibrated, which confirms that the experiment was realized in almost ideal conditions with respect
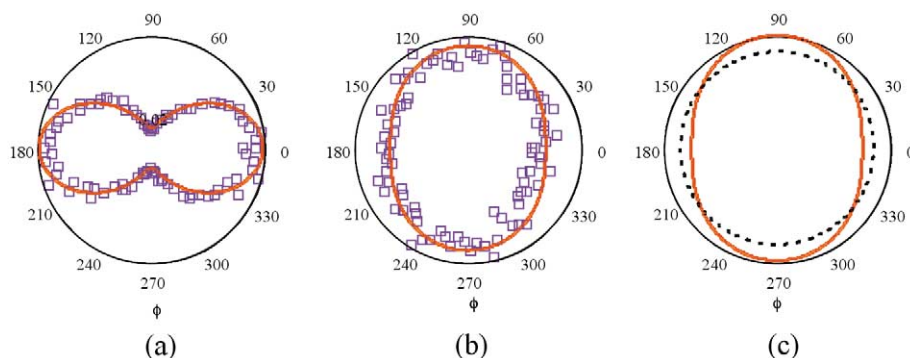
Figure 6. Experimental SHG (a) and THG (b) intensities responses (squares) as functions of a variable incoming reading polarization in the sample plane. The experiment has been performed using a grafted DR1-PMMA polymer (5% w/w), and parallel writing-beam polarizations during 30 minutes. The corresponding fits (continuous lines) provide parameters for the molecular anisotropy: $\|\beta^3\|/\|\beta^1\| = 0.45$ (SHG), and for the one photon to two-photon excitation efficiency: $p_1 = 0.17$ and $p_3 = 0.27$ (THG). (c) The theoretical fit of the photoinduced THG anisotropy (continuous line) is confronted to the initial isotropic circular THG response (dashed line).

to optimal poling efficiency. From the experimental p_1 and p_3 values, it is possible to further infer an order of magnitude for the joint one- and two-photon excitation efficiency p_2. Assuming $\phi_1 = \phi_2 = \phi_3$ and taking DR1 polarizabilities values as published in the literature, the resolution of the set of equations (5) gives $p_2 \approx 0.08$. This means that the joint one- and two-photon excitation is lower in efficiency, but still in the same magnitude range as the other effects, which is a prerequisite towards all-optical poling optimization.

In theory, by measuring the molecular hyperpolarisabilities and the fields intensity with increased precision, it is possible to infer from such experiments the complete three-dimensional photoinduced molecular distribution, while the data collected here have permitted a more limited, albeit insightful, access to the centrosymmetric and non-centrosymmetric parts of $f(\Omega)$. Further studies to fully unveil the rotational spectrum of $f(\Omega)$ are currently in progress.

5. Conclusions

The all-optical poling technique in molecular media is the only orientation process that allows to tailor adjustable multipolar patterns in the molecular orientation distribution function. The underlying process is rather complex but depends only, at equilibrium, on molecular polarizabilities and write field tensor symmetries. We have presented here the possibility to design both write and read-out tensorial processes in order to answer a diversity of important issues ranging from holographic polarization storage to determination of molecular distribution function or insights into molecular polarizability symmetries. Using all-optical poling, the second and third nonlinear processes have been used in order to provide information on the odd and even orders of the molecular distribution function, up to the 4th order. Along similar lines, higher order interactions in the material, such as a conjunction between one- and three-photon absorptions, can provide order parameter beyond $J = 4$. This work has demonstrated a possible experimental insight into the symmetry of the orientational distribution of molecules in photo-oriented thin films, with implications as to on-going research involving molecular nonlinear photonics in thin films [23] and microcavities [24].

References

[1] H. Le Bozec, T. Le Bouder, O. Maury, A. Bondon, I. Ledoux, S. Brasselet, J. Zyss, Supramolecular octupolar self-ordering towards nonlinear optics, Adv. Mater. 13 (2001) 1677–1681.

[2] J. Zyss, A. Donval, P. Labbé, E. Toussaere, Nonlinear photonic engineering: physics and applications, in: E. Maroni, A. Frieseni (Eds.), Unconventional Optical Elements for Information, Kluwer, 2000, pp. 109–126.

[3] J. Zyss, I. Ledoux, Nonlinear optics in multipolar media: theory and experimental, Chem. Rev. 4 (1994) 77–105.
[4] J. Zyss, S. Brasselet, Nonlinear photonic engineering: from NLO as a goal to NLO as a tool, C. R. Acad. Sci. Paris Sér. IV 1 (2000) 601–608.
[5] M. Dumont, A. El Osman, On spontaneous and Photoinduced orientational mobility of dye molecules in polymers, Chem. Phys. 245 (1999) 437–447.
[6] R.J. Glauber, in: R.J. Glauber (Ed.), Quantum Optics, Proc. E. Fermi Internat. School in Physics, Academic Press, New York, 1967, p. 15.
[7] U. Osterberg, W. Margulis, Opt. Lett. 12 (1987) 57–59.
[8] N.B. Baranova, B.Ya. Zel'dovich, Physical effects, in optical fields with nonzero average cube $\langle E^3 \rangle \neq 0$, J. Opt. Soc. Am. B 8 (1) (1991) 27–32.
[9] C. Fiorini, F. Charra, J.M. Nunzi, Six wave mixing probe of light-induced second-harmonic generation: example of dye solution, J. Opt. Soc. Am. B 11 (12) (1994) 2347–2358.
[10] S. Brasselet, J. Zyss, Control of the photoinduced micro-patterning of nonlinear organic thin films: from molecular to photonic engineering, J. Opt. Soc. Am. B 15 (1) (1998) 257–288.
[11] C. Fiorini, F. Charra, J.M. Nunzi, I.D.W. Samuel, J. Zyss, Light-induced second-harmonic generation in an octupolar dye, Opt. Lett. 20 (24) (1995) 2469–2471.
[12] V. Blanchet, C. Nicole, M. Bouchene, B. Girard, Temporal control in two-photon transitions: from optical interferences to quantum interferences, Phys. Rev. Lett. 78 (14) (1997) 2716–2719.
[13] D. Meshulach, Y. Silberberg, Coherent quantum control of multiphoton transitions by shaped ulstrashort optical pulses, Phys. Rev. A 60 (2) (1999) 1287–1292.
[14] J.T. William, Angular Momentum, Wiley Interscience, 1994.
[15] J. Zyss, S. Brasselet, Multipolar symmetry patterns in molecular nonlinear optics, J. Nonlinear Opt. Phys. Mater. 7 (3) (1998) 397–439.
[16] J. Jerphagnon, D.S. Chemla, R. Bonneville, The description of the physical properties of condensed matter using irreducibel tensors, R. Adv. Phys. 27 (1978) 609–650.
[17] J. Zyss, Molecular engineering implication of rotational invariance in quadratic nonlinear optics: from dipolar to octupolar molecules and materials, J. Chem. Phys. 98 (1993) 6583–6599.
[18] S. Bidault, S. Brasselet, J. Zyss, Symmetry effects in coherent control of molecular orientations in polymers using multiphotonic excitation pathways, in preparation.
[19] S. Brasselet, J. Zyss, Control of the polarization dependence of optically poled nonlinear polymer films, Opt. Lett. 22 (19) (1997) 1464–1466.
[20] R. Bonneville, Symmetries of the light scattering processes in low-density fluids, Phys. Rev. A 17 (6) (1978) 2046–2061.
[21] B. Boulanger, J. Zyss, in: A. Authier (Ed.), Physical Properties of Crystals, International Tables for Crystallography, Vol. D, 1996.
[22] V.M. Churikov, C.C. Hsu, Optical control of third-harmonic generation in azo-doped polymethylmethacrylate thin films, Appl. Phys. Lett. 77 (14) (2000) 2095–2097.
[23] Xiuqin Yu, Xiaoxia Zhong, Qu Li, Shouyu Luo, Yingli Chen, Yu Sui, Jie Yin, Method for improving optical poling efficiency in polymer films, Opt. Lett. 26 (4) (2001) 220–222.
[24] R. Piron, E. Toussaere, D. Josse, S. Brasselet, J. Zyss, Towards nonlinear photonics in all-optically poled polymer microcavities, Synth. Met. 115 (2000) 109–119.